Kinetics of Hydrogen Absorption in a Stirred Metal Hydride Slurry

Isothermal, isobaric measurements were made of the rate of hydrogen absorption by a slurry of $LaNi_5$ powder suspended in *n*-undecane in a baffled stirred reactor. The data were interpreted using a model embodying three resistances in series: a gas-liquid mass transfer resistance, a liquid-solid mass transfer resistance, and an "overall reaction resistance."

At the highest agitator speeds employed, 2,000 rpm, conversions of $LaNi_5$ to hydride of 90% or better were obtained within one minute or less, thereby confirming the potential of the metal hydride slurry concept for commercial applications.

Yuanki Tung, E. W. Grohse,
F. B. Hill
Brookhaven National Laboratory
Upton, NY 11973

SCOPE

Metal hydrides and their formers have been under study for some years as hydrogen-absorbing media. [Strictly speaking, hydrogen is absorbed by a metal hydride former, such as lanthanum nickel-five ($LaNi_5$), also called the α-solid phase, to form a metal hydride, such as lanthanum nickel-five hexahydride ($LaNi_5H_6$), called the β-solid phase. Upon heating and/or lowering the pressure of the latter, it is transformed back to the metal hydride former, with the release (desorption) of hydrogen. However, in common discussions of these phenomena, distinction between metal hydrides and their formers is omitted and the simple term, metal hydride, is used for both, as in the present paper.]

The large capacity of metal hydrides for hydrogen storage coupled with their ready release of hydrogen at moderate temperatures and pressures and their ability to undergo many cycles of absorption and desorption with little decrease in capacity, have prompted examination of their usefulness in a variety of industrial applications. These include hydrogen storage in energy conversion cycles, chemical heat pumps and compressors, hydrogen purification, and hydrogen isotope separation.

Two properties of metal hydrides have been found to be of critical importance in the design of reactor vessels containing metal hydrides, usually in granule or powder form, in which the absorption and desorption of hydrogen is alternately carried out:

1. The tendency of the hydride particles to fragment during successive absorption-desorption cycles, resulting in the production of undesirably fine powders after only a few cycles, with appreciable changes in bed volume.
2. Appreciable heats of hydriding (absorption) and dehydriding (desorption).

In the case of $LaNi_5$ ($LaNi_5H_x$), the latter amounts to approximately 30 kJ/mol of hydrogen. In conventional gas-solid beds, this fragmentation property requires special designs to deal with the resulting settling and compaction, and consequent deformation and hydrogen flow distribution problems in the containment vessels. Also, in gas-solid beds the large heats of hydriding and dehydriding require complicated facilities for the removal and addition of heat, respectively, and/or long absorption and desorption times in order to avoid excessive bed temperature gradients within the bed, which would result in incomplete absorptions and desorptions and consequently reduced sorbent utilization.

One remedy for these problems has been proposed

The permanent address of Yuanki Tung is: Institute of Chemical Metallurgy, Chinese Academy of Sciences, Beijing, China.

The present address of E. W. Grohse is: E. W. Grohse Associates, Port Jefferson Station, NY 11776.

by Rudman et al. (1983). These investigators use proprietary pelleted forms of a given hydride former in admixture with an inert material, usually a metal. The inert material serves as a thermal ballast and limits the temperature rise during absorption (or lowering during desorption). The pelleted forms are further alleged to have good resistance to fragmentation.

In the present study, an alternative first proposed by Winsche in 1973 (Grohse and Reilly, 1982) was employed in order to avoid the above problems, namely, the use of slurries of metal hydride particles suspended in an inert liquid or so-called solvent. In a slurry reactor, particle fragmentation cannot cause vessel deformation, although the possibilities of inadequate suspension or particle carry-over by entrainment must be properly handled in the design of such reactors. Problems such as restricted access of hydrogen to particles due to compacting in gas-solid systems are immediately eliminated in well-agitated gas-liquid-solid systems. [Gas-solid and gas-liquid-solid systems are also referred to as two-phase and three-phase systems, respectively. This terminology will also be followed in the present paper although, strictly speaking, three and four phases, respectively, are involved. That is, there are two solid phases—α and β solid phases—in addition to the liquid and/or gas phase.] In particular, temperature gradients within properly designed slurry reactors are negligible compared to those within gas-solid systems. On the other hand, in gas-slurry reactors liquid mass transfer resistances adjacent to the gas and solid phases are introduced; these resistances can be minimized by adequate agitation. Also, there is the possibility that the adsorption of solvent molecules upon the surfaces of the suspended particles may introduce additional mass transfer as well as reaction resistances that, in turn, may further impede the adsorption and dissociation of hydrogen on these surfaces.

Until recently, all studies of metal hydride-hydrogen applications have been based on the use of gas-solid reactors. The practical feasibility of slurry hydride reactors was first demonstrated by Grohse and Reilly in 1982 when it was shown that $LaNi_{4.5}Al_{0.5}$ powders suspended in 2,2,4 trimethylpentane ("isooctane") exhibited the same equilibrium dissociation pressure-composition isotherm relationship as a dry $LaNi_{4.5}Al_{0.5}$ system, provided that account was taken of the vapor pressure of the suspending liquid. Initial kinetic studies were performed by Reilly et al. (1982) and a patent application relating to the use of metal hydride slurries has been submitted by Reilly et al. (1983). Further kinetics studies have been and are being carried out by Reilly and Johnson (1984).

The present study was undertaken to determine rates of hydrogen absorption in $LaNi_5$/*n*-undecane slurries in a turbine-agitated baffled autoclave to determine the relative influences of the mass transfer and reaction processes, and to determine the effect of the solvent phase on the kinetics of the reaction between hydrogen and the solid phase.

CONCLUSIONS AND SIGNIFICANCE

Rates of absorption of hydrogen in a suspension of $LaNi_5$ in *n*-undecane determined experimentally in a small baffled stirred autoclave were found to increase with hydrogen pressure and with stirrer speed and to exhibit a maximum with respect to temperature, all as expected. Contrary to expectations, the rate increased moderately with solid phase loading, presumably because of unavoidable variations in the activation procedure. Multiple activation steps were required both in the dry state and after solvent addition in order to obtain useful reproducibility.

The absorption rate data were used to test a model of the combined mass transfer and reaction phenomena present in the slurry reactor. The model takes into account the liquid phase resistances adjacent to the interfaces with the gas and solid phases and an overall reaction resistance that takes into account all other possible mass transfer and reaction resistances. The fit of the model to the data was good in response to variations of pressure, stirrer speed, and temperature.

The model was used to estimate values of the overall reaction rate constant. Required in the calculation of this constant were values of the gas-liquid mass transfer resistance obtained from separate experiments, and values of the liquid-solid mass transfer resistance obtained from the correlation of Harriott (1962). The latter resistance was determined to be negligible and the overall reaction rate constants were found to be independent of hydrogen pressure and stirrer speed, as expected.

This work increases the basis of understanding of rate phenomena in metal hydride slurries. Also, it presents a mathematical model of slurry reactor performance that should be useful for prediction purposes. The practical usefulness of metal hydride slurries as an alternative to gas-solid reactors may thereby be enhanced.

Introduction

The present work is concerned with the kinetics of absorption of hydrogen by a slurry of $LaNi_5$ suspended in *n*-undecane and thus involves the study of a three-phase gas-liquid-solid system. With one exception, to be described below, no other kinetic studies have been reported on three-phase metal hydride systems.

When a "chemically inert" solvent such as *n*-undecane is interposed between the hydrogen and solid phases, mass transfer resistances within the solvent are introduced and the observed rate of hydrogen absorption decreases, for a given overall concentration driving force. A simplified schematic representation of the concentration profile in a slurry reactor resulting from the mass transfer resistances in the solvent as well as from the surface and reaction processes associated with gas-solid systems (Goodell and Rudman, 1983) is shown in Figure 1. As shown for the solvent phase in this figure, there are liquid-side resistances adjacent to both the gas-liquid interface and the liquid-solid interface. No resistance is introduced on the gas side of the gas-liquid interface when the gas phase is pure hydrogen. Also, in a gas-liquid-solid system there is the likelihood of a tightly packed multilayer of liquid molecules existing on the solid surface. These molecules must be displaced before molecular hydrogen can reach active chemisorption and dissociation sites. This would provide additional mass transfer resistances, and there is also the possibility of exchange reactions between hydrogen atoms and the adsorbed liquid hydrocarbon molecules, which might result in additional reaction resistances. In Figure 1 these additional surface resistances are not shown, and in the mathematical model proposed these additional resistances would be included within the overall reaction resistance characterized as $k_R a_S$ in Eq. 9. Quantitative consideration of these additional phenomena is presently underway.

Two questions immediately arise with respect to hydrogen absorption kinetics when a third (liquid) phase, is added:

1. How is the intrinsic reaction rate to be deduced from an observed rate influenced by mass transfer processes in the third phase?

2. How is the intrinsic rate affected by the presence of the third phase?

The one other kinetics study of the H_2–*n*-undecane–$LaNi_5$ system was conducted recently by Reilly and Johnson (1984). They measured rates of hydrogen absorption in a baffled stirred reactor. The stirrer was a Teflon-coated bar magnet, the rotating motion of which was induced by a driving rotating magnet external to and below the reactor. For each experiment, the absorption rate was obtained from the approximately straight-line, central portion of the sigmoid-shaped fractional conversion vs. time curve, and this rate was used to evaluate the constants in the equation

$$R_{RJ} = A_{RJ} \exp\left(-Q_{RJ}/R_O T\right)\left(p_G - p_A\right) \tag{1}$$

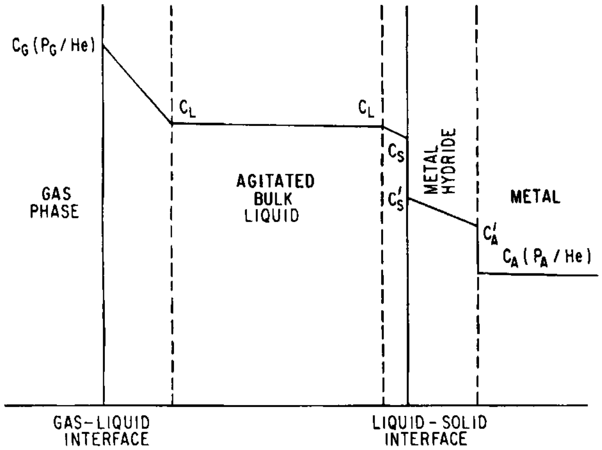

Figure 1. Concentration profile in stirred slurry reactor.

Also measured by Reilly and Johnson in the same apparatus were rates of hydrogen absorption in *n*-undecane in the absence of $LaNi_5$. These rates, expressed as mass transfer coefficients, could be described by

$$k_L a_L = A_L \exp\left(-Q_L/R_O T\right) \tag{2}$$

The corresponding pairs of numerical values of the constants in Eqs. 1 and 2, i.e., A_{RJ} and A_L, on the one hand, and Q_{RJ} and Q_L on the other, were found to be very nearly equal. Hence the absorption rate in the presence of $LaNi_5$ was deduced to be controlled by the mass transfer resistance at the gas-liquid interface, attributable to the considerably smaller agitator power inputs achievable in the Reilly-Johnson apparatus as compared to the present apparatus. This result, therefore, precluded obtaining answers to the questions just previously raised.

The present work was undertaken to address those questions. Specifically, a program of experiments was carried out and an interpretation scheme devised to permit deduction of intrinsic reaction rate constants from the experimental data.

Absorption Rate Equations

Two series of experiments were carried out in the present study. The first involved measurement of rates of absorption of hydrogen in *n*-undecane in the absence of $LaNi_5$. A falling-pressure technique was used for this purpose, and gas-liquid mass transfer coefficients were calculated from the data obtained. In the second series of experiments, rates of absorption of hydrogen in $LaNi_5$–*n*-undecane slurries were measured. A constant-pressure technique was used and intrinsic reaction rate constants for the absorption of hydrogen by $LaNi_5$ were calculated from the data, as discussed below. Rate equations to describe and interpret these experiments are presented in this section. Experimental details are given later.

Absorption in n*-undecane*

In this series of experiments, hydrogen was absorbed from a high-purity hydrogen phase into the low vapor pressure inert solvent, *n*-undecane with $LaNi_5$ absent. The initial hydrogen content of the solvent was zero. The gas phase pressure transient can be described by the following expression equating the rate of loss of hydrogen from the gas phase to its rate of entry into the well-mixed liquid phase

$$-\frac{V_G}{R_O T_G}\frac{dp_G}{dt} = k_L a_L V_L \left(\frac{p_G}{He} - c_L\right) \tag{3}$$

with the initial conditions

$$t = 0, \quad p_G = p_i, \quad c_L = 0 \tag{4}$$

A material balance for hydrogen in the gas and liquid phases is

$$\frac{V_G}{R_O T_G}\frac{dp_G}{dt} + V_L\frac{dc_L}{dt} = 0 \qquad (5)$$

with the same initial conditions. Upon integrating these equations, the following equation relating the gas phase pressure transient to the gas-liquid mass transfer coefficient, $k_L a_L$, can be obtained

$$\ln\frac{p - p_f}{p_i - p_f} = -k_L a_L \frac{p_i}{p_f} t \qquad (6)$$

Using Eq. 6, $k_L a_L$ is determined from the slope of a plot of experimental data in the form $\ln [(p - p_f)/(p_i - p_f)]$ vs. time.

Absorption in $LaNi_5$–n-undecane slurry

In this series of experiments, hydrogen was continuously supplied to the reactor from a reservoir of known volume through a constant downstream pressure regulating valve. The rate of hydrogen uptake was determined by measuring the pressure transient in the reservoir. In developing a model describing these experiments, the following simplified sequence of rate phenomena was assumed:

1. Transfer of hydrogen from the gas-liquid interface to the bulk liquid.
2. Transfer from the well-mixed bulk liquid to the surfaces of the suspended solid particles.
3. An overall reaction process associated with the solid phase which, following terminology commonly used for gas-solid systems, may also be referred as the overall intrinsic rate process for a gas-liquid-solid system.

In a gas-solid system, the first two phenomena are nonexistent, and the overall intrinsic rate process consists of a minimum of the following subprocess occurring at the surfaces and within the solid phase:

(a) Chemisorption of molecular hydrogen and dissociation of the latter to atomic hydrogen.

(b) Diffusion of atomic hydrogen through the β-phase to the α-phase/β-phase boundary.

(c) Transformation of metal hydride former to metal hydride at this boundary.

Goodell and Rudman (1983) refer to the sequence of phenomena included in subprocess (a) as the surface process, and combine processes (b) and (c) into a single "bulk process."

In a gas-liquid-solid system, what has been referred to above as the overall reaction process may include, in addition to the above subprocesses inherent in a gas-solid system, other mass transfer and reaction resistances associated with the physical adsorption of liquid molecules upon the solid surfaces. In the mathematical model development that follows, an overall intrinsic *reaction* rate process characterized by the term $k_R a_S$ is assumed.

An expression equating the rate of loss of hydrogen from the reservoir to its rate of entry into the well-mixed liquid phase is

$$-\frac{V_R}{R_O T_R}\frac{dp_R}{dt} = k_L a_L V_L\left(\frac{p_G}{He} - c_L\right) \qquad (7)$$

An expression equating the rate of entry of hydrogen into the liquid phase to the sum of its rate of transfer to the solid surface and its rate of accumulation in the liquid is

$$k_L a_L V_L\left(\frac{p_G}{He} - c_L\right) = k_S a_S V_L(c_L - c_S) + V_L\frac{dC_L}{dt} \qquad (8)$$

The rate of transfer of hydrogen to the solid surface is equal to the rate of reaction of hydrogen with the solid which, in turn, is equal to the rate of accumulation of hydrogen in the hydride formed:

$$k_S a_S V_L(c_L - c_S) = k_R a_S V_L\left(\frac{H}{M}\right)_f \cdot f(F)\cdot\left(c_S - \frac{p_A}{He}\right) = \frac{3W}{M_M}\left(\frac{H}{M}\right)_f \frac{dF}{dt} \qquad (9)$$

where

$$F = (H/M)/(H/M)_f$$

$$f(F) = 3(1 - F)\,[-\ln(1 - F)]^{2/3} \qquad (10)$$

$$k_R = A_R \exp(-Q_R/R_O T) \qquad (11)$$

The reaction rate term in Eq. 9 involves the conversion-dependent factor $f(F)$ given by Rudman (1983) for a three-dimensional nucleation and growth process, and a linear concentration difference, $c_S - p_A/He$.

An overall hydrogen balance is

$$\frac{V_R}{R_O T_R}\frac{dp_R}{dt} + V_L\frac{dc_L}{dt} + \frac{3W}{M_M}\left(\frac{H}{M}\right)_f\frac{dF}{dt} = 0 \qquad (12)$$

The initial conditions for Eq. 12 are

$$t = 0,\quad p_R = p_O,\quad c_L = 0,\quad F = 0 \qquad (13)$$

With these initial conditions, the integrated form of Eq. 12 becomes

$$\frac{V_R}{R_O T_R}(p_O - p_R) = V_L c_L + \frac{3W}{M_M}\left(\frac{H}{M}\right)_f F \qquad (14)$$

Equations 7 and 8 and the two equations composing Eq. 9 constitute a system of four equations in the four dependent variables $k_R a_S$, c_L, c_S, and F. The material balance equation, Eq. 12, may be derived by summing Eqs. 7–9 and is thus not an independent equation. It is nevertheless a useful relation as will be seen later when data reduction is discussed.

A number of limiting cases of the applicable differential equations are also of interest.

Negligible Liquid-Solid Mass Transfer Resistance. When $k_S a_S$ is large, $c_S \approx c_L$, and the system of equations becomes

$$-\frac{V_R}{R_O T_R}\frac{\mathrm{d}p_R}{dt} = k_L a_L V_L\left(\frac{p_G}{He} - c_L\right) \qquad (7)$$

$$k_La_LV_L\left(\frac{p_G}{He}-c_L\right)=k_Ra_SV_L\left(\frac{H}{M}\right)_f \cdot f(F)\cdot\left(c_L-\frac{p_A}{He}\right)+V_L\frac{dc_L}{dt} \quad (15)$$

$$k_Ra_SV_L\left(\frac{H}{M}\right)_f\cdot f(F)\cdot\left(c_L-\frac{p_A}{He}\right)=\frac{3W}{M_M}\left(\frac{H}{M}\right)_f\frac{dF}{dt} \quad (16)$$

These equations assume only a gas-liquid resistance and an overall (intrinsic) reaction resistance, and are referred to as the two-resistance model, whereas the full system of equations constitutes the three-resistance model.

Gas-Liquid Mass Transfer Resistance Dominant. When k_La_L is small and both k_Sa_S and k_Ra_S are large, then $c_L \approx p_A/He$, $dC_L/dt \approx 0$, and the system of equations reduces to

$$-\frac{V_R}{R_OT_R}\frac{dP_R}{dt}=k_La_LV_L\left(\frac{p_G}{He}-\frac{p_A}{He}\right)=\frac{3W}{M_M}\left(\frac{H}{M}\right)_f\frac{dF}{dt} \quad (17)$$

This is the equation used by Reilly and Johnson (1984) to interpret their data.

Reaction Resistance Dominant. When k_Ra_S is small, the rate of loss of hydrogen from the reservoir is determined by the gas-solid reaction rate. Thus

$$-\frac{V_R}{R_OT_R}\frac{dP_R}{dt}=k_Ra_SV_L\left(\frac{H}{M}\right)_f\cdot f(F)\left(\frac{p_G}{He}-\frac{p_A}{He}\right)=\frac{3W}{M_M}\left(\frac{H}{M}\right)_f\frac{dF}{dt} \quad (18)$$

Experimental

Apparatus

Hydrogen absorption experiments were carried out in a 150 mL stainless steel autoclave provided with a leak-tight, magnetically driven stirrer (Autoclave Engineers model ABP-300). Details of construction and principal dimensions are shown in Figure 2. The stirrer was a disc turbine with six flat blades located at approximately the mid-height of the liquid phase. The stirrer shaft was magnetically coupled to a variable-speed drive and was equipped with gas-lubricated graphite bearings. The stirrer shaft was hollow and was provided with holes located in the gas and liquid phases as shown. By means of this arrangement, at sufficiently high stirrer speeds hydrogen could be drawn from the gas space directly into the liquid at the plane of the rotating impeller, thereby providing direct dispersion of hydrogen bubbles into the liquid phase. A single baffle was provided.

A schematic diagram of the entire apparatus is shown in Figure 3. The reactor was immersed in a constant temperature bath controllable to within 0.5 K. The two lines were connected to the reactor, one for admission of *n*-undecane from a burette and another for admission of hydrogen or helium or for evacuation of the reactor. A 600 mL reservoir used in the isobaric experiments supplied hydrogen to a pressure regulator which, in turn, supplied hydrogen at a constant pressure to the reactor.

Falling-pressure experiments

In conducting a falling-pressure experiment for the determination of volumetric gas-to-liquid mass transfer coefficients, k_La_L, the burette was filled with *n*-undecane (466–468 K boiling point range). The solvent was degassed by bubbling helium of 99.995% purity through the undecane for approximately 5 min. After allowing all bubbles to disengage from the liquid, 100 mL of the degassed solvent was drawn into the evacuated reactor. The reactor was now pressurized with hydrogen of 99.999% minimum purity to a predetermined initial pressure and then isolated. The stirrer was started, and the ensuing pressure transient, as sensed by a Dynisco pressure transducer, was automatically recorded. A fresh charge of solvent was used for each of the falling pressure experiments.

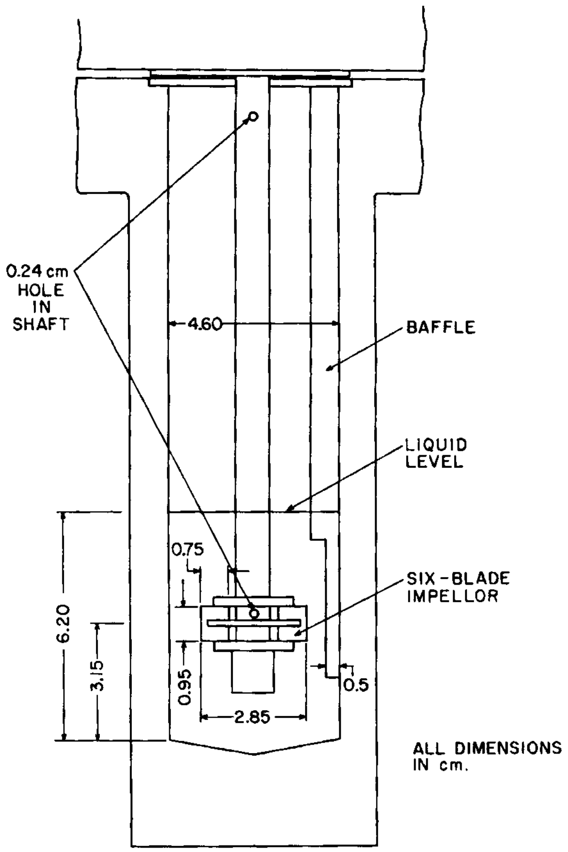

Figure 2. Stirred slurry reactor.

Constant-pressure experiments

In conducting a series of constant-pressure experiments with a given constant loading of metal hydride, a weighed quantity of −75 mesh $LaNi_5$ (HY-STOR 205 alloy, Heat No. T-28107, MPD Technology Corp.) was charged to the dry reactor. After closing the reactor, the $LaNi_5$ charge was activated in the following manner. The reactor was evacuated, charged with helium at a pressure slightly above atmospheric pressure, and then heated for 5 min to approximately 403 to 433 K by means of a hand-held hot air blower. The reactor was then allowed to cool to approximately 323 K and finally evacuated again for approximately 15 min, achieving an ultimate absolute pressure of 10 to 20 millitorr (1.33 to 2.66 Pa).

Hydrogen was then introduced and initially maintained overnight at a pressure of approximately 10.9 atm (1.10 MPa). The evacuation and pressurization steps were then repeated approximately ten times, each step requiring 3 to 4 h. This procedure

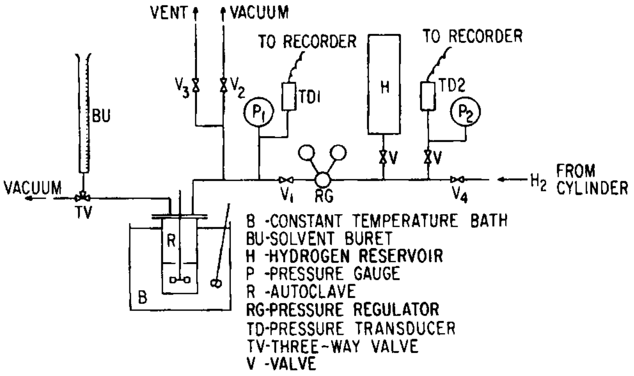

Figure 3. Apparatus diagram.

has been shown to provide rapid rates of hydrogen absorption and an ultimate $LaNi_5$ average particle size of the order of 20 μm (Belkbir et al., 1979).

After activating the dry $LaNi_5$ charge, 100 mL of degassed *n*-undecane was transferred to the evacuated reactor. Then after charging the reservoir, hydrogen was introduced into the reactor (initially under vacuum) at a regulated constant pressure. There was first an immediate, abrupt small drop in the reservoir pressure as the reactor became pressurized. After a few seconds, the stirrer, which cannot be operated under a vacuum, was started, thereby initiating a continuous falling off of the reservoir pressure as hydrogen was absorbed by the slurry. This pressure transient was automatically recorded. After absorption of hydrogen was completed, hydrogen was slowly vented from the reactor. Then the reactor was slowly evacuated in preparation for the run to follow.

When the constant-pressure series of runs was begun, it was quickly determined that in spite of the $LaNi_5$ having been thoroughly activated in the dry state (as previously described), after the addition of carefully degassed *n*-undecane additional activation was still required before reproducible data could be obtained. That is, absorption data appeared reproducible only after an additional nine cycles of hydriding (pressurization) and dehydriding (evacuation) in the presence of solvent. And even after these additional measures, some drifting of the data was still observed, as discussed later.

All experiments at a given $LaNi_5$ loading were carried out with a single charge of $LaNi_5$ and a single charge of *n*-undecane. At the conclusion of a series of experiments with a given $LaNi_5$ loading, approximately 98 mL of solvent free of solids was recovered from the reactor, with a small additional amount of solvent still adhering to the solids. Thus, less than 2% of a solvent charge was lost to the vacuum system during a series of such experiments. Also, after completion of each set of experiments at a given loading, the $LaNi_5$ was recovered for BET surface area measurement.

Auxiliary experiments were also carried out in order to determine:

1. The minimum agitator speed required for complete suspension of the $LaNi_5$ powder in the solvent
2. The minimum speed required for the injection of gas bubbles into the solvent
3. The settling time for the slurry particles.

These experiments were carried out with the head of the autoclave reactor and its integral stirrer and baffle inserted into a glass reactor body of the same internal dimensions as that of the stainless steel body, using the same volume of *n*-undecane but using air at atmospheric pressure instead of hydrogen at an elevated pressure.

Available and estimated physical properties of *n*-undecane and $LaNi_5$ are given in Table 1.

Results and Discussion

Auxiliary experiments

The minimum speed required to achieve complete and visually uniform suspension of 15 g of powdered $LaNi_5$ in 100 mL of *n*-undecane was approximately 300 rpm. This powder charge was close to the maximum subsequently used in the constant-pressure experiments. It was assumed that this stirrer speed would likewise produce complete suspension of slightly larger as well as smaller charges.

The minimum speed required for the injection and dispersion of air bubbles into the solvent at atmospheric pressure and room temperature was approximately 530 rpm. The number of bubbles increased with increasing speed above the minimum, while the size of the bubbles appeared to remain approximately the same.

The settling time for the smallest observable particles in the slurry was approximately 90 s. This time corresponds to a Stokes law particle diameter of approximately 10 μm.

BET surface areas for the three loadings used averaged $0.34 \pm 0.02\ m^2 \cdot g^{-1}$.

Absorption of hydrogen in n*-undecane (falling-pressure experiments)*

Typical plots of reactor pressure vs. time for these experiments, of the form predicted by Eq. 6, are shown in Figure 4 for

Table 1. Properties of *n*-Undecane and $LaNi_5$

Temp. K	Density g/cm³*	Viscosity cp**	Diffusivity cm²/s†	Vapor Press. kPa‡	Plateau Press. kPa‡	Henry's Constant kPa/(mol/cm³)‡
303	0.734	1.00	7.5×10^{-5}	0.114	301	2.96×10^7
313	0.726	0.87	9.1×10^{-5}	0.212	444	2.82×10^7
323	0.718	0.76	1.09×10^{-4}	0.378	638	2.69×10^7
333	0.711	0.67	1.29×10^{-4}	0.650	897	2.58×10^7

*From *International Critical Tables*, 3, 30, McGraw-Hill, New York (1928).

**Estimated via Akgerman and Gainer (1972) method, using reference value at 20°C from *Handbook of Physics and Chemistry*. SI conversion: mPa · s = cp.

†Calculated from correlation of Akgerman and Gainer (1972).

‡Calculated from correlations given by Reilly and Johnson (1984).

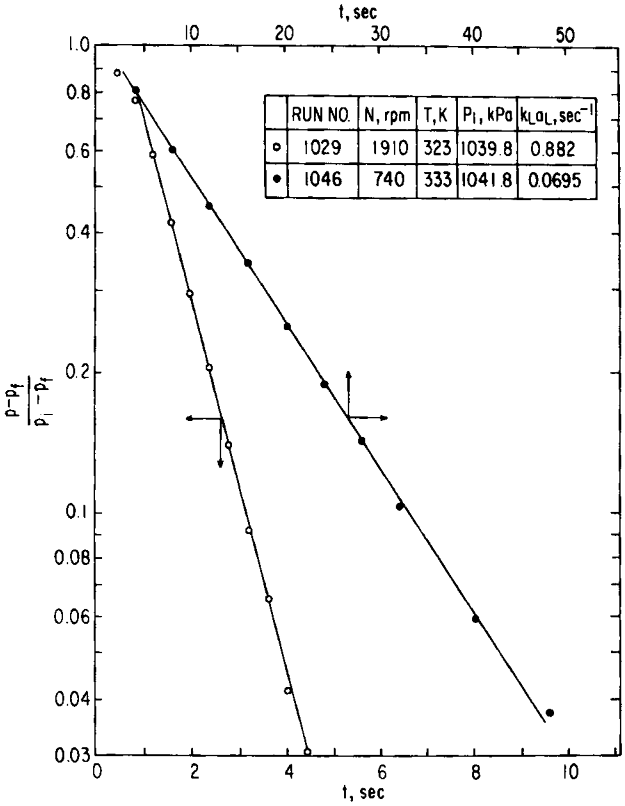

Figure 4. Pressure transients in absorption of H_2 by *n*-undecane in baffled stirred reactor.

two stirrer speeds but with otherwise essentially identical conditions. Both stirrer speeds shown are above the minimum required for the dispersion of air bubbles. The straight lines fitted to the data in Figure 4 do not intersect the ordinate at $(p_G - p_f)/(p_i - p_f)$ when $t = 0$ as predicted by theory, presumably because of the finite time required to pressurize the reactor and the necessity of delaying starting the stirrer for a second or two until the reactor was pressurized. The slopes of the straight lines from which the values of k_La_L were calculated were nevertheless reproducible.

Values of k_La_L calculated from such plots are summarized in Figure 5 for all the experiments performed. At a given temperature, k_La_L is essentially zero at stirrer speeds below which gas bubbles were injected and dispersed into the solvent during the tests using air. Measurable values of k_La_L are first observed at stirrer speeds exceeding 500 rpm. At higher stirrer speeds, k_La first increases gradually with stirrer speed and then increases much more rapidly and linearly. At a given stirrer speed, k_La_L increases with temperature. As the data for 300 K indicate, k_La_L does not vary significantly with initial pressure nor with the presence of loadings of added stainless steel powder approximating up to twice the loadings of $LaNi_5$ subsequently employed; see Figure 5. Stainless steel is inert to hydrogen at the conditions used.

The variation of k_La_L with stirrer speed is believed to be due primarily to the increase in the number of bubbles (and, hence, in a_L) with stirrer speed, as observed in the experiments conducted with the glass reactor body. As previously mentioned, the bubble size appeared essentially independent of stirrer speed. By itself, k_L does not vary strongly with stirrer speed (Sherwood et al., 1975). The increase of k_La_L with temperature corresponds to an activated process with $Q_L/R_0 = 1{,}300$ K, a value in the range observed for diffusion-limited phenomena. The behavior of k_La_L shown in Figure 5 is similar to that found by others, e.g., Westerterp et al. (1963) and Mehta and Sharma (1971).

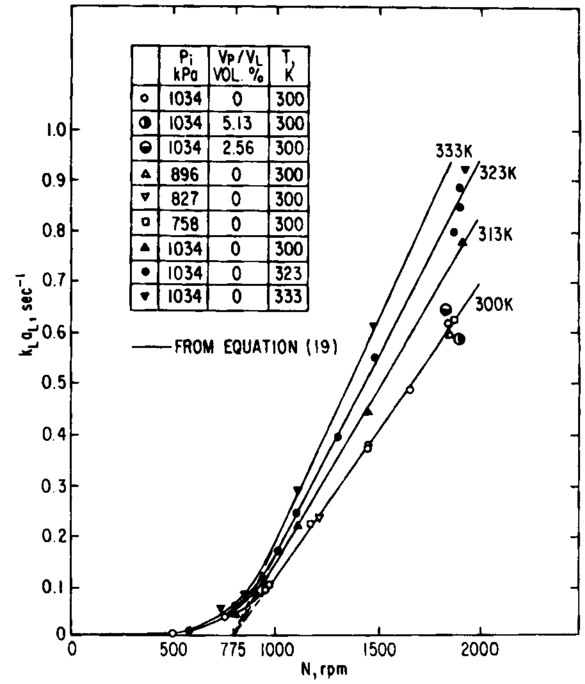

Figure 5. Liquid-side mass transfer coefficients for absorption of H_2 by *n*-undecane in baffled stirred reactor.

The linear portions of the curves in Figure 5 when extrapolated intersect in a common point, $N_0 = 775$ rpm at $k_La_L = 0$. With this observation, the linear portions of these curves for the range of temperatures studied can be represented by the following equation

$$k_La_L = 4.07 \times 10^{-4} \cdot \exp[0.0127\,(T - 273)]\,(N - 775) \quad (19)$$

Absorption of hydrogen in the $LaNi_5$–n-undecane slurry (constant-pressure experiments)

Data from the experiments with slurries showing the effects of absorption pressure, stirrer speed, and temperature are shown in Figures 6–8 as plots of fractional conversion vs. time. Fractional conversions were calculated from the reservoir pressure transients as follows. Using Eq. 7 and values of dp_R/dt obtained by numerical differentiation of the pressure transient data, c_L was calculated as a function of time. Then using Eq. 14, corresponding values of F were calculated.

The resulting sigmoid-shaped curves of F vs. t shown in Figures 6–8 are typical of many gas-solid reactions and especially of hydrogen-metal reactions (Belkbir et al., 1979). The rate of hydrogen absorption is seen to increase with pressure and stirrer speed and to go through a maximum with temperature. This kind of temperature dependence results from the plateau pressure increasing with temperature, thereby reducing the driving force term, $c_S - p_A/He$, while at the same time the temperature-

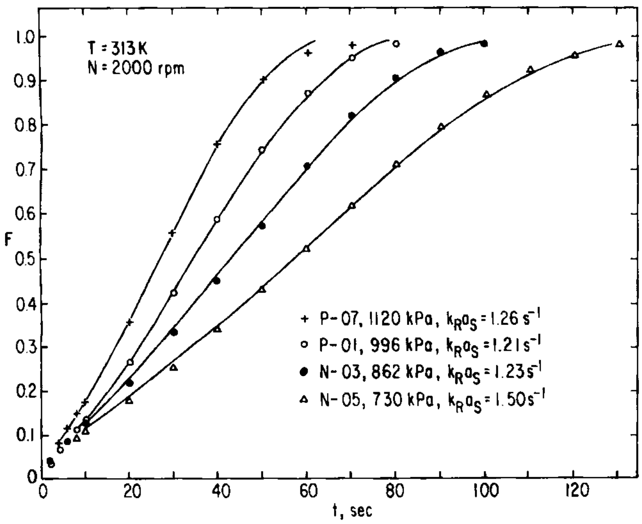

Figure 6. Effect of pressure on rate of conversion of $LaNi_5$ to $LaNi_5H_6$ in baffled stirred slurry reactor.

dependent rate constant, k_R, increases. This kind of temperature dependence has been reported by others, e.g., Goodell and Rudman (1983).

The rate equations presented earlier for the three-resistance model, Eqs. 7–9, can be used in the following way to deduce values of the overall reaction rate constant from the data. The parameter k_La_L is evaluated using Eq. 19 and the parameter k_Sa_S is calculated from Harriott's (1962) correlation. With the parameters k_La_L and k_Sa_S in hand, k_Ra_S is selected as that value which on numerical integration of Eqs. 7–9 gives the curve of best fit to the fractional conversion-time data in Figures 6–8. In addition, as a test of the relative importance of the liquid-solid resistance compared to the other resistances, the equations for the two-resistance model were used in the same way for a selected number of experiments.

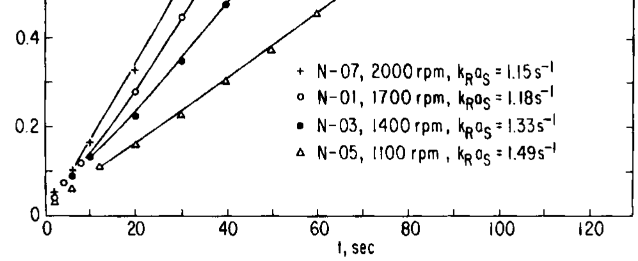

Figure 7. Effect of stirrer speed on rate of conversion of $LaNi_5$ to $LaNi_5H_6$ in baffled stirred slurry reactor.

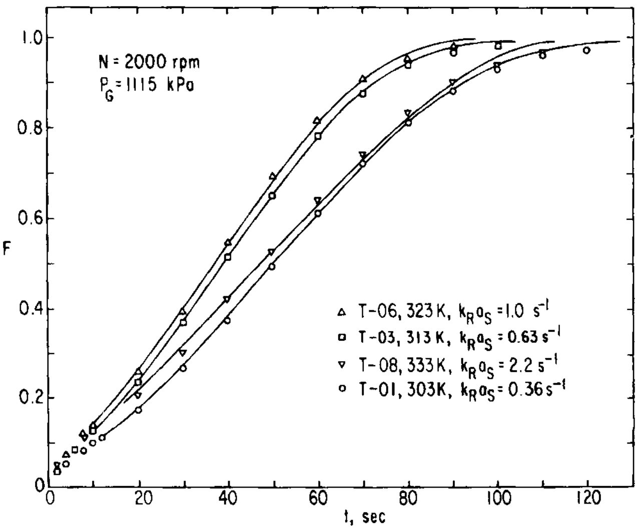

Figure 8. Effect of temperature on rate of conversion of $LaNi_5$ to $LaNi_5H_6$ in baffled stirred slurry reactor.

In using this procedure, k_Sa_S was estimated using a particle size of 20 μm, based upon the findings of Belkbir et al. (1979) for $LaNi_5$ following repeated activations. However, the results of the procedure were found not to change appreciably as a result of using a considerably smaller particle size. For example, using what is believed to be an unrealistically small particle size of 2 μm, corresponding to a BET surface area of 0.3 m^2/g, did not significantly affect the values of k_Ra_S obtained. The diffusivity of hydrogen in *n*-undecane required in the calculation of k_Sa_S was estimated using the correlation of Akgerman and Gainer (1972). The Henry's law constants for H_2 in *n*-undecane and absorption plateau pressure isotherms for $LaNi_5$ were taken from Reilly and Johnson (1984). A density of 7.8 g · cm^{-3} was used for $LaNi_5$.

Standard numerical integration techniques were used for integration of Eqs. 7–9 or Eqs. 7, 15, and 16. Each integration was started at the value of F corresponding to $H/M \approx 0.1$. The initial conditions for the other variables, p_R, c_L, and c_S, were the values calculated to correspond to $H/M \approx 0.1$. This procedure was followed because at H/M less than ≈ 0.1, hydrogen dissolution occurs in the α-solid phase without the formation of the second, β-solid phase (see explanation of phases in Scope section), for which the proposal model does not apply. (Hydride formation occurs at values of H/M greater than approximately 0.1.) For example, the reaction rate term in Eq. 9 would predict zero reaction rate at zero conversion, a physically unacceptable situation. The practice of integrating the applicable system of rate equations starting at a fractional conversion greater than zero has also been followed by others; e.g., Jacobs and Ng (1972), Nakamori et al. (1974).

The solid curves shown in Figures 6–8 represent the best fit to the experimental data obtained by the above procedure. The fit is seen to be good using either model and is sensitive in the last reported decimal place. The values of k_Ra_S corresponding to the best fit are presented in two columns in Table 2. The first listing was obtained using the three-resistance model, and the second listing was obtained using the two-resistance model. It is seen that very little, if any, change results from neglecting the liquid-solid resistance, thereby indicating that this resistance is negligible. Note also in this connection that the values of $k_S a_S$ listed in Table 2 are between 15 and 100 times as great as the corresponding values of $k_L a_L$. On the other hand, the gas-liquid mass transfer resistance is important and dominates at low stirrer speeds, as indicated in Figure 9. The equation applicable when this resistance dominates, Eq. 17, is seen to be a fair approximation to the experimental data for 1,100 rpm but is a poor representation of the data for 2,000 rpm.

Figure 10 is an Arrhenius plot of $k_R a_S/W$, a quantity proportional to the reaction rate constant, k_R. (k_R by itself cannot be calculated from $k_R a_S$ since a_S is not known; however, since W is proportional to a_S, then $k_R a_S/W$ is proportional to k_R.) Solid phase loading, W/V_L, is the parameter in Figure 10. The values of Q_R/R_O indicated in the figure for the different loadings are identical for the 10 and 20 g loadings, 5,670 K, and just a little less for the 5 g loading, 5,070 K. (Evidently by coincidence, the arithmetic average value for the three loadings, 5,470 K, is almost identical to that determined for the bulk process postulated by Goodell and Rudman, 1983, for their two-phase hydrogen absorption experiments, 5,480 K.) While $k_R a_S/W$ is shown to increase somewhat with loading, the increase is believed to be due primarily to experimental variations, particularly in the activation process. In principle, no plausible explanation is known for an increase with loading. It should be noted that

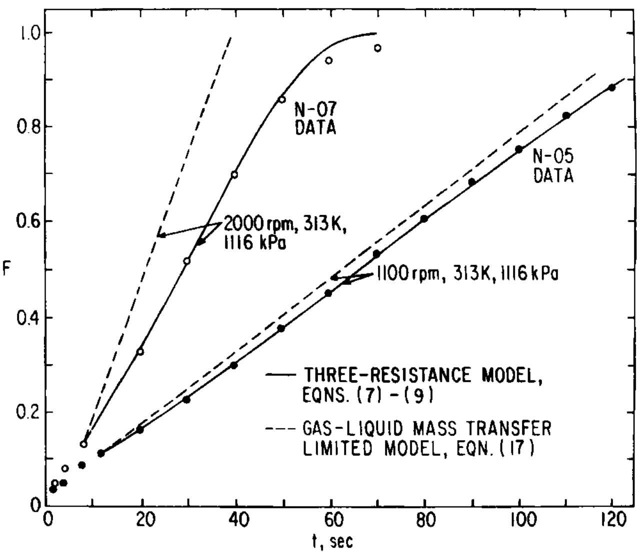

Figure 9. Comparison of gas-liquid mass-transfer limited model and model including reaction resistance with experimental data.

Table 2. Kinetics of Absorption of Hydrogen in $LaNi_5$ Slurries

Run No.	W g	T_R K	P_G kPa	N rpm	$(H/M)_f$ $\frac{\text{Atoms } H_2}{\text{Atoms metal}}$	$k_L a_L$ s^{-1}**	$k_S a_S$ s^{-1}***	$k_R a_S$ s^{-1}†	$k_R a_S$ s^{-1}‡	$k_R a_S/W$ $g^{-1} \cdot s^{-1}$†
T-01	10	303	1,130	2,000	0.973	0.7298	22.15	0.36	—	0.036
T-02	10	303	1,117	2,000	0.991	0.7298	22.15	0.36	0.36	0.036
T-03*	10	313	1,120	2,000	0.946	0.8286	27.23	0.63	0.62	0.063
T-04*	10	313	1,120	2,000	0.941	0.8286	27.23	0.63	—	0.063
T-05	10	323	1,117	1,950	0.908	0.9024	32.85	1.0	1.0	0.10
T-06	10	323	1,120	1,980	0.915	0.9255	33.0	1.0	—	0.10
T-07	10	333	1,120	2,000	0.899	1.068	39.89	1.9	1.9	0.19
T-08	10	333	1,120	2,000	0.861	1.068	39.89	2.2	—	0.22
T-09*	10	313	1,117	2,010	0.908	0.8354	27.27	0.95	0.95	0.095
T-10*	10	313	1,117	2,000	0.913	0.8286	27.23	0.96	—	0.096
P-01	10	313	996	1,980	0.914	0.8151	27.15	1.21	1.21	0.121
P-02	10	313	996	2,000	0.921	0.8286	27.23	1.23	—	0.123
P-03	10	313	862	2,000	0.899	0.8286	27.23	1.23	1.23	0.123
P-04	10	313	862	1,980	0.885	0.8151	27.12	1.37	—	0.137
P-05	10	313	730	2,000	0.89	0.8286	27.23	1.50	1.46	0.150
P-06	10	313	725	2,000	0.894	0.8286	27.23	1.51	—	0.151
P-07*	10	313	1,120	2,010	0.91	0.8354	27.23	1.26	—	0.126
N-01	10	313	1,117	1,700	0.934	0.6257	25.92	1.18	1.16	0.118
N-03	10	313	1,117	1,400	0.91	0.4228	24.46	1.33	—	0.133
N-05	10	313	1,116	1,110	0.913	0.2198	22.81	1.49	1.45	0.149
N-07*	10	313	1,116	2,000	0.934	0.8286	27.23	1.15	—	0.115
C5-3	5	303	1,148	1,960	1.12	0.706	11.23	0.18	0.18	0.036
C5-4	5	313	1,149	1,965	1.11	0.8049	13.89	0.29	—	0.058
C5-5	5	323	1,147	1,940	1.1	0.8947	16.81	0.44	—	0.088
C5-6	5	333	1,146	1,935	1.07	1.012	20.24	0.83	—	0.17
C20-3	20	303	1,117	2,010	0.882	0.7357	44.35	0.90	0.90	0.045
C20-4	20	313	1,130	2,020	0.883	0.8421	54.6	1.6	—	0.080
C20-5	20	323	1,116	1,995	0.869	0.937	66.11	2.7	—	0.14

*Runs with nominally identical conditions: 313 K, 1,120 kPa, 2,000 rpm, 10 g $LaNi_5$.

**Calculated using Eq. 19.

***Calculated from correlation of Harriott (1962).

†Calculated using three-resistance model, Eqs. 7, 8, and 9.

‡Calculated using two-resistance model, Eqs. 7, 15, and 16.

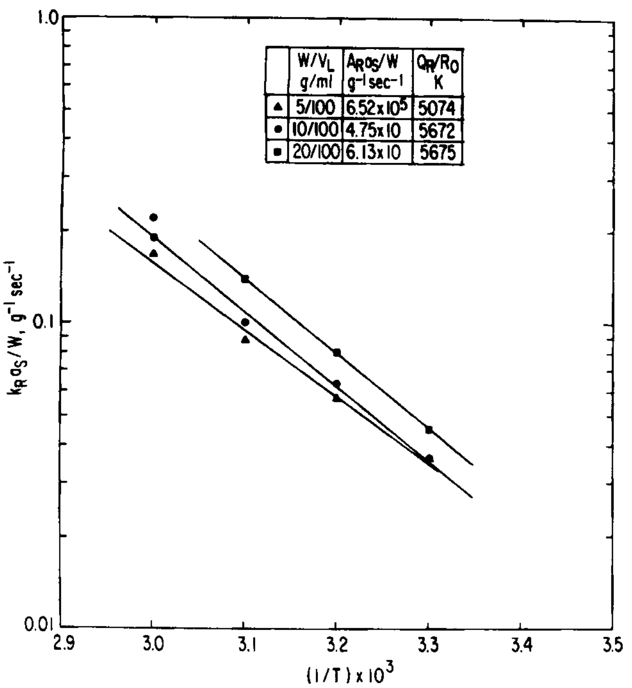

Figure 10. Arrhenius plot of $k_R a_S/W$ with solid phase loading as a parameter.

Reilly and Johnson (1984) found no increase in rate with loading.

As mentioned in the Experimental section, multiple activation steps were used for $LaNi_5$ in the dry state, in accordance with normal practice, and additional activation steps were required after solvent addition in order to obtain acceptable reproducibility. Even after both procedures, an upward drift of rates persisted initially but finally leveled off. Thus, the runs in Table 2 are listed in the order in which they were performed. The runs identified with an asterisk were all performed at nominally the same conditions of temperature (313 K), pressure (1,120 kPa), stirrer speed (2,000 rpm), and $LaNi_5$ loading (10 g). The average value of $k_R a_S$ for these runs was 0.93 s^{-1}, with a range of -32% (0.63 s^{-1}) to $+35\%$ (1.26 s^{-1}). Reflected in this range are effects of all sources of experimental variability but especially the variations in effectiveness of activation procedures. It is felt that runs performed in close succession with a single loading of $LaNi_5$ for the purpose of determining the influence of a given variable—e.g., temperature, pressure, or stirrer speed—were minimally influenced by a drift in activity. Runs performed with different loadings, on the other hand, are likely to exhibit maximum differences stemming from activity differences.

By means of Eq. 18, several values of $R_{0.5}$ ($= d(H/M)/dt$ at $H/M = 0.5$) were calculated in order to compare intrinsic reaction rates attainable in a gas-liquid-solid system if sufficient agitation were available to eliminate all liquid phase mass transfer resistances with intrinsic rates obtained by Goodell and Rudman for a gas-solid system at comparable temperatures and pressures. This comparison is shown in Table 3. The much lower values obtained for the gas-liquid-solid system are in part attributable to the substantial agitation provided in this study still not being sufficient to essentially eliminate the gas-liquid mass transfer resistance (it having previously been shown that the liquid-solid resistance is negligible), but these values appear primarily attributable to the existence of additional resistances at the solid surfaces owing to the adsorption of solvent molecules on the surfaces.

Table 3. Comparison of Hydrogen Absorption Rates in $LaNi_5$ Slurry Systems and Dry Systems

	$[d(H/M)/dt]$ at $H/M = 0.5$, min^{-1}		
Reaction Conditions	Exp.	Calc. Eq. 18	Dry System
Slurry, 1,120 kPa, 313 K, 2,000 rpm	1.0*	2.0	95†
Slurry, 1,033 kPa, 313 K, 1,200 rpm	0.3**	—	98†

*This work.
**Reilly and Johnson (1984).
†Goodell and Rudman (1983).

Goodell and Rudman (1983) made extensive measurements of the intrinsic rate of the H_2-$LaNi_5$ reaction as a function of temperature and pressure. Using a nonlinear regression technique, they then fitted their data to the proposed two-resistance model (surface and bulk resistances) previously mentioned. The data obtained in the present study were insufficient in number to perform a similar analysis with useful precision.

Acknowledgment

The authors express appreciation to J. J. Reilly, J. R. Johnson, H. C. Cheng, and J. W. Sutherland for helpful discussions and to S. Bookless for experimental assistance. This work was supported by the Division of Chemical Sciences, U.S. Department of Energy, under Contract No. DE-AC02-76CH00016.

Notation

A_L = frequency factor in definition $k_L a_L = A_L \exp(-Q_L/R_O T)$, s^{-1}
A_R = frequency factor in definition $k_R = A_R \exp(-Q_R/R_O T)$, cm · s^{-1}
A_{Rj} = frequency factor, Eq. 5, mol · s^{-1} · kPa^{-1}
a_L = specific surface area of bubbles per unit volume of liquid phase, cm^{-1}
a_S = specific surface area of particles per unit volume of liquid phase, cm^{-1}
c_L = hydrogen concentration in bulk liquid, mol · cm^{-3}
c_S = hydrogen concentration in liquid phase contiguous to surface of particles, mol · cm^{-3}
c_S' = effective hydrogen concentration on surface of particle, mol · cm^{-3}
F = fractional conversion, dimensionless
He = Henry's law constant, kPa · cm^3 · mol^{-1}
$(H/M)_f$ = final equilibrium atomic ratio of hydrogen-to-metal in solid phase, dimensionless
k_L = gas-liquid mass transfer coefficient, cm · s^{-1}
k_R = intrinsic reaction rate constant, cm · s^{-1}
k_S = liquid-solid mass transfer coefficient, cm · s^{-1}
M_M = molecular weight of $LaNi_5$ (432.46)
N = agitator speed, rpm
N_o = x-intercept, Eq. 19
p_A = plateau pressure, kPa
p_f = final pressure in falling-pressure experiment, kPa
p_G = hydrogen pressure of gas phase in reactor, kPa
p_i = initial pressure in falling-pressure experiment, kPa
p_O = initial pressure in reservoir, kPa
p_R = hydrogen pressure in reservoir, kPa
p_s = effective pressure on particle surface, kPa
Q_L/R_O = activation energy for gas-liquid mass transfer, K
Q_R/R_O = activation energy for intrinsic reaction, K

Q_{RJ}/R_O = activation energy, Eq. 1, K
R_{RJ} = reaction rate, Eq. 1, mol · s^{-1}
R_O = universal gas constant, 8.3145 J · mol^{-1} · K^{-1}
T = reaction temperature, K
T_G = gas phase temperature in reactor, K
T_R = reservoir temperature, K
t = time, s
V_G = volume of gas phase in reactor, cm^3
V_L = volume of liquid phase in reactor, cm^3
V_P = volume of particles, cm^3
V_R = reservoir volume, cm^3
W = weight of particles, g

Literature cited

Akgerman, A., and J. L. Gainer, "Diffusion of Gases in Liquids," *Ind. Eng. Chem. Fundam.*, **11**, 373 (1972).

Belkbir, L., N. Gerard, A. Percheron-Guegan, and J. C. Achard, "Kinetics of Hydrogen Absorption and Desorption by Ternary $LaNi_5$-type Intermetallic Compounds," *Int. J. Hydrogen Energy*, **4**, 541 (1979).

Goodell, P. D., and P. S. Rudman, "Hydriding and Dehydriding Rates of the $LaNi_5$-H System," *J. Less Common Metals*, **89**, 117 (1983).

Grohse, E. W., and J. J. Reilly, "Feasibility of Metal Hydride Slurry Systems," Dept. Appl. Sci., Brookhaven Nat. Lab., Upton, NY (1982).

Harriott, P., "Mass Transfer to Particles. I: Suspended in Agitated Tanks," *AIChE J.*, **8**, 93 (1962).

Jacbos, P. W. M., and W. L. Ng, "Reactivity of Solids," *Proc. 7th Int. Symp. on Reactivity of Solids*, Chapman and Hall, London (1972).

Mehta, Z. E., and M. M. Sharma, *Chem. Eng. Sci.*, **26**, 461 (1971).

Nakamori, I., O. H. Nakamura, and T. Hayano, "Thermal Decomposition and Reduction of Silver Oxide," *Bull. Chem. Soc. Japan*, **47**, 1827 (1974).

Reilly, J. J., E. W. Grohse, and J. R. Johnson, "Metal Hydride Slurries," *Proc. Condensed Papers, 5th Miami Int. Conf. Alt. Energy Sources*, T. N. Veziroglu, ed., Univ. Miami, Coral Gables, FL (1982).

Reilly, J. J., E. W. Grohse, and W. Winsche, "Liquid Suspensions of Reversible Metal Hydrides," U.S. Patent Appl., Brookhaven Nat. Lab., Upton, NY (1983).

Reilly, J. J., and J. R. Johnson, "The Kinetics of the Absorption of Hydrogen by $LaNi_5H_x$/*n*-Undecane Suspension," *J. Less Common Metals*, **90** (1984).

Rudman, P. S., "Hydriding and Dehydriding Kinetics," *J. Less Common Metals*, **89**, 93 (1983).

Rudman, P. S., Sandrock, and P. D. Goodell, "Hydrogen Separation from Gas Mixtures Using $LaNi_5$ Pellets," *J. Less Common Metals*, **89**, 437 (1983).

Sherwood, T. K., R. L. Pigford, and C. R. Wilke, *Mass Transfer*, McGraw-Hill, New York (1975).

Westerterp, K. R., L. L. Van Dierendonck, and J. A. de Kraa, "Interfacial Areas in Agitated Gas-Liquid Contactors," *Chem. Eng. Sci.*, **18**, 157 (1963).

Manuscript received Nov. 5, 1985, and revision received Mar. 3, 1986.